Catalysis Today 187 (2012) 159–167

Contents lists available at SciVerse ScienceDirect

Catalysis Today

journal homepage: www.elsevier.com/locate/cattod

Catalytic properties of new ternary Nb-Sb-V oxide – A comparative study with mechanical mixture of single oxides and binary systems

Maria Ziolek[1,*], Hanna Golinska-Mazwa[1], Elzbieta Filipek[2,**], Mateusz Piz[2]

[1] Adam Mickiewicz University, Faculty of Chemistry, Grunwaldzka 6, 60-780 Poznan, Poland
[2] West Pomeranian University of Technology, Szczecin, Faculty of Chemical Technology and Engineering, al. Piastów 42, 71-065 Szczecin, Poland

ARTICLE INFO

Article history:
Received 26 July 2011
Received in revised form 18 October 2011
Accepted 19 October 2011
Available online 1 December 2011

Keywords:
Nb-Sb-V-oxides
2-Propanol decomposition
Acetonylacetone cyclisation
Methanol oxidation

ABSTRACT

The study presents a comparative analysis of catalytic properties of new Nb_2SbVO_{10} ternary oxide against those of a mechanical mixture of single oxides and a mixture of single with binary oxide, all of the same chemical composition. Moreover, the material without antimony (Nb_9VO_{25}) was tested. Acid–base and redox properties were studied in the following test reactions: 2-propanol decomposition, acetonylacetone (AcOAc) cyclisation and methanol oxidation. The properties of ternary oxide and the mechanical mixture of single oxides are not significantly different. The main difference is in the generation of more active Lewis acid–base pairs in ternary oxide, which is demonstrated by the higher production of ether in the intermolecular dehydration of 2-propanol. Acidic/basic and redox properties of the oxide catalysts containing Nb, Sb, V, O (atomic ratio: 2:1:1:10) strongly depend on the presence of binary oxide, which significantly enhances the basicity of the catalysts. The highest basicity was found for pure binary oxide Nb_9VO_{25} but this catalyst without Sb exhibits much lower activity in the transformation of both alcohols.

1. Introduction

Vanadium oxide-based catalysts are used industrially in several important processes. Among them bulk V_2O_5 is used in the oxidation of SO_2 to SO_3 for the production of sulphuric acid and in the oxidation of benzene to maleic acid, mixed V-Mo oxides for the oxidation of naphthalene to phthalic anhydride, $V_2O_5/WO_3/TiO_2$ for selective reduction of NOx with ammonia [1]. Most catalysts based on vanadium oxide consist of vanadium oxide loaded on different supports (usually metal oxide supports). Different compositions of multicomponent metal oxides containing vanadium oxide species have been tested. Rutile SbVOx based catalysts are of a great interest for ammoxidation processes [2–6]. They have also been found attractive in selective oxidation of methanol. Li et al. [7] have used $VSbOx/SiO_2$ for methanol oxidation to formaldehyde and found that Sb-V mixed oxides are more selective than vanadia supported on silica because the relative amount of monomeric VOx species is higher in mixed oxides. Various metal oxides and mixed metal oxides have been already used in methanol oxidation. It has been frequently observed that the addition of the second oxide which is itself inactive or unselective for the oxidation reaction substantially improves the activity of the primary oxide [7]. Such inactive oxide exhibiting donor properties is Sb_2O_4. Delmon et al. [8] described spillover of oxygen adsorbed dissociatively on Sb_2O_4 from which oxygen atoms diffuse to the primary oxide (in their work it was SnO_2). The same phenomenon can be expected if another metal oxide like V_2O_5 or Nb_2O_5 is used as acceptor oxide.

It has been evidenced by the literature data [1,9–12] that the activity of oxide catalysts in oxidation of methanol and also in several other oxidation processes is related to vanadium species, but different mixed metal oxides and additives play a crucial role in enhancement of activity and directing the catalytic reactions to desired products. Recently, the Sb-V-Nb systems ($SbVO_4$/NbSiOx) were applied in the oxidation of methanol [13]. It has been documented that the presence of niobium in the support for rutile $SbVO_4$ decreases the acidity of SbVOx leading to ether production and increases the selectivity to formaldehyde.

In this work we would like to answer the question of what is the role of vanadium, antimony and niobium mixed oxides in the acid/base and redox catalytic properties. Our interest was to test a new composite ternary oxide described in [14] containing V, Nb and Sb in methanol oxidation and also in two other reactions applied for acid–base tests, i.e. 2-propanol decomposition and acetonylacetone (AcOAc) cyclisation. Of particular interest was a comparison of the catalytic properties of mechanically mixed: (i) V, Sb, Nb single oxides; (ii) Sb-V binary and Nb single oxides; and (iii) ternary Nb_2SbVO_{10} compound, all of the same chemical composition. Moreover, the material without antimony (Nb_9VO_{25}) was prepared by heating a mixture of V_2O_5 and T-Nb_2O_5 at the molar

* Corresponding author. Tel.: +48 61 8291243.
** Corresponding author.
E-mail addresses: ziolek@amu.edu.pl (M. Ziolek), elafil@zut.edu.pl (E. Filipek).

0920-5861/$ – see front matter © 2011 Elsevier B.V. All rights reserved.
doi:10.1016/j.cattod.2011.10.038

Table 1
Phase composition, atomic ratio and weight percentage of vanadium, antimony, and niobium in the catalysts.

Catalysts	Phase composition	Mol. content [%]	V:Sb:Nb atomic ratio	V [wt.%]	Sb [wt.%]	Nb [wt.%]
Nb,Sb,V-O10	V_2O_5	25.00	1:1:2	9.98	23.85	18.20
	T-Nb_2O_5	50.00				
	α-Sb_2O_4	25.00				
Nb,(Sb-V)-O10	$SbVO_5$	50.00	1:1:2	9.82	23.48	17.92
	T-Nb_2O_5	50.00				
(Nb-Sb-V)-O10	Nb_2SbVO_{10}	100.00	1:1:2	9.82	23.48	17.92
(Nb-V)-O25	Nb_9VO_{25}	100.00	1:0:9	3.96	–	64.97

ratio of 1:9 according to [15]. All samples prepared were characterized and tested in the reactions mentioned above.

2. Experimental

2.1. Preparation of the materials

The following compounds were used in preparation procedures: orthorhombic V_2O_5 a.p. (POCh, Poland), orthorhombic T-Nb_2O_5 a.p. (Sigma–Aldrich, Germany), orthorhombic α-Sb_2O_4 obtained by heating in air the commercial Sb_2O_3 a.p. (Merck, Germany). Moreover, $SbVO_5$, Nb_2SbVO_{10} and Nb_9VO_{25} compounds were prepared from oxides by the methods described in [14–16]. The compounds were obtained as a result of heating of the appropriate stoichiometric mixtures of oxides V_2O_5, T-Nb_2O_5 and α-Sb_2O_4 according to the equations:

$$V_2O_{5(s)} + Sb_2O_{4(s)} + 1/2O_{2(g)} = 2SbVO_{5(s)} \quad (1)$$

$$Nb_2O_{5(s)} + SbVO_{5(s)} = Nb_2SbVO_{10(s)} \quad (2)$$

$$V_2O_{5(s)} + 9Nb_2O_{5(s)} = 2Nb_9VO_{25(s)} \quad (3)$$

Reactions nos. (1)–(3) were carried out by the conventional method by calcination of mixtures of oxides in air, at temperatures not exceeding 923, 973 and 1273 K, respectively. The starting mixtures of substrates (1–3) after mechanical homogenization by grinding in an agate mortar and shaping them into pellets were heated at a few stages. After each heating stage the samples were gradually cooled to room temperature, weighed, homogenized by triturating and shaped again into pellets before the subsequent heating stage. Heating of the reaction mixtures was finished when the obtained samples contained only monophases of $SbVO_5$, Nb_2SbVO_{10} or Nb_9VO_{25}.

The following mechanical mixtures were used in this study: (i) 25 mol% V_2O_5, 50 mol% T-Nb_2O_5 and 25 mol% alfa-Sb_2O_4 – labelled in this work as **Nb,Sb,V-O10**; (ii) 50 mol% $SbVO_5$ and 50 mol% T-Nb_2O_5 – labelled as **Nb,(Sb-V)-O10**. Moreover, Nb_2SbVO_{10} sample (labelled as **(Nb-Sb-V)-O10**) was prepared according to Eq. (2). Finally, the material Nb_9VO_{25} (labelled as **(Nb-V)-O25**) was obtained by heating of a mixture of V_2O_5 and T-Nb_2O_5 at the molar ratio of 1:9 (Eq. (3)).

The description of all the samples used as catalysts is shown in Table 1.

The catalysts used for further study were homogenized by grinding in an agate mortar (Pulverisette 2, FRITSCH) in three 15-min cycles.

2.2. Characterization of catalysts

2.2.1. X-ray diffraction (XRD)

X-ray diffraction patterns of catalysts were recorded on a HZG4/A2 (Carl Zeiss, Germany) diffractometer using CuKα radiation (λ = 0.15418 nm) and Ni filter. Working conditions were 40 kV, 30 mA, and the scanning rate of 0.02°/s for Bragg's angles (2θ) from 10 to 50. The phases in the samples were identified on the basis of their XRD characteristics from PDF cards [Powder Diffraction File, International Centre for Diffraction Data (Swartmore, USA, 1989)] and papers [14,17].

2.2.2. Scanning electron microscopy (SEM)

Scanning electron microscopy study was performed on JSM-1600, Jeol, Japan with an X-ray energy dispersive analysis – EDX (ISIS-300, Oxford).

2.2.3. Ultraviolet–visible spectroscopy

UV–Vis spectra were recorded on a Varian-Cary 300 Scan UV–visible spectrophotometer with an integrated sphere CA-30I. Catalysts, dehydrated at 673 K for 2 h, in the form of powders were placed into a cell equipped with a quartz window. The Kubelka–Munk function (F(R)) was used to convert reflectance measurements into equivalent absorption spectra using the reflectance of SPECTRALON as a reference.

2.2.4. Infrared spectroscopy study

The phase composition of the samples was also evaluated before and after methanol oxidation on the basis of FTIR spectra measured for a mixture of 4 mg of the catalysts and 200 mg of dehydrated KBr pressed into a pellet. Bruker Vector 22 FT-IR spectrometer (resolution 4 cm^{-1}) was applied.

2.3. Test reactions

The catalysts were pressed (under pressure of ~20 MPa) and granulated to 0.5 < Ø < 1 mm size fraction before each test reaction.

2.3.1. Acetonylacetone cyclisation

The catalysts were tested in acetonylacetone (AcOAc) cyclisation. A tubular, down-flow reactor (Ø 8 mm; length 80 mm) was used for AcOAc cyclisation reaction that was carried out at atmospheric pressure, using nitrogen as the carrier gas. The catalyst bed (0.1 g, 2 mm height in the reactor) was first activated for 2 h at 673 K (heating rate 15 K/min) under nitrogen flow (40 cm^3 min^{-1}). Subsequently, a 0.5 cm^3 of acetonylacetone (Fluka, GC grade) was passed continuously into the catalyst at 623 K. The substrate was delivered with a pump system (KD Scientific) and vaporized before being passed through the catalyst with the flow of nitrogen carrier gas (40 cm^3 min^{-1}). The reaction products were collected for 30 min downstream of the reactor in a cold trap (liquid nitrogen + 2-propanol) and analysed by gas chromatography (SRI 310 C, MXT®-1 column 30 m, temperature of column 373 K) with TCD detector. Helium was applied as a carrier gas.

2.3.2. 2-propanol decomposition

The 2-propanol dehydration and dehydrogenation was performed using a microcatalytic pulse reactor (Ø 6 mm; length 80 mm) inserted between the sample inlet and the column of a CHROM-5 chromatograph. A portion of 0.1 g (3 mm height in the reactor) of granulated catalyst was activated at 673 K (heating rate 10 K/min) for 2 h under helium flow (40 cm^3 min^{-1}). The

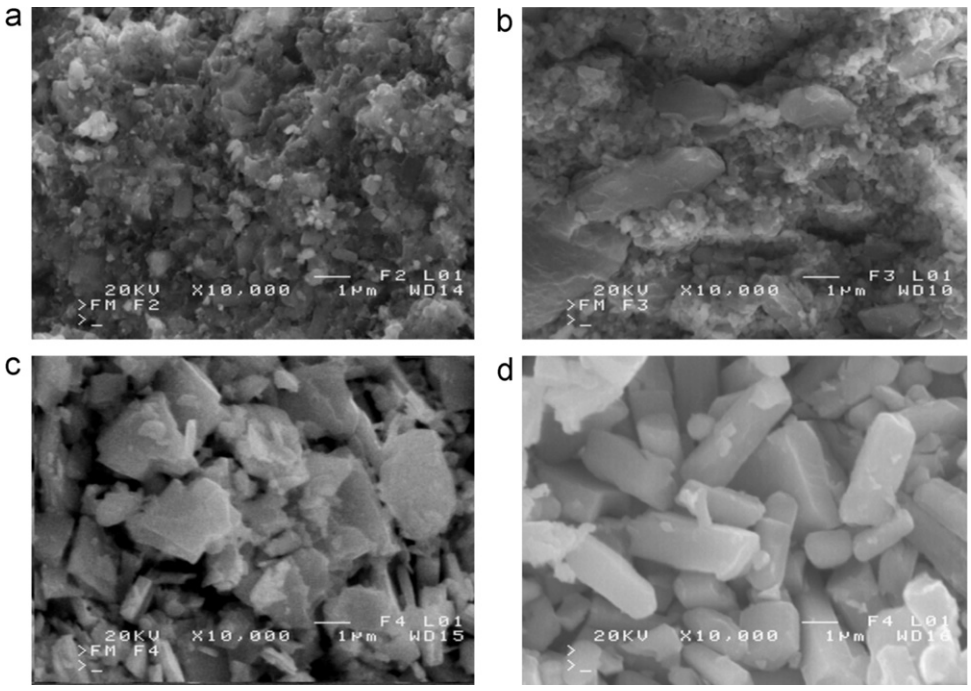

Fig. 1. SEM images of catalysts used: (a) Nb,Sb,V-O10, (b) Nb,(Sb-V)-O10, (c) (Nb-Sb-V)-O10, (d) (Nb-V)-O25.

2-propanol (Chempur, Poland) conversion was studied at various temperatures using 3 μl pulses of alcohol under helium flow (40 cm^3 min^{-1}). The substrate was vaporized before being passed through the catalyst bed with the flow of helium carrier gas. The products: propene, 2-propanone (acetone) and diisopropyl ether were identified by CHROM-5 gas chromatograph on-line with microreactor. The reaction mixture was separated on 2 m column filled with Carbowax 400 loaded on Chromosorb W (80-100 mesh) at 338 K in helium flow (40 cm^3 min^{-1}) and detected by TCD.

2.3.3. Methanol oxidation

The methanol oxidation reaction was performed in a fixed-bed flow reactor. A portion of 0.1 g (4 mm height in the reactor) of pure (undiluted) was placed in the reactor (Ø 5 mm; length 70 mm). The samples were activated in argon flow (40 cm^3 min^{-1}) at 673 K for 2 h (the rate of heating was 15 K/min). Then temperature was decreased to that of the reaction. The reactant mixture of Ar/O_2/MeOH (88/8/4 mol%) was supplied at the rate of 40 cm^3 min^{-1} for standard reactions. Methanol (Chempur, Poland) was introduced to the flow reactor by bubbling argon gas through a glass saturator filled with methanol. The reaction was conducted at GHSV = 80 000 h^{-1} g^{-1}_{cat}. The reactor effluent was analysed using an on-line two gas chromatographs. One chromatograph GC 8000 Top equipped with a capillary column of DB-1 operated at 313 K – FID detector was applied for analyses of organic compounds and the second GC containing and Porapak Q and 5A molecular sieves columns for analyses of O_2, CO_2, CO, H_2O and CH_3OH – TCD detector). The columns in the second chromatograph with TCD were heated according to the following program: 5 min at 358 K, increase of the temperature to 408 K (heating rate 5 K/min), 4 min at 408 K, cooling down to 358 K (for the automatic injection on the column with 5A), 10 min at 358 K, increase of the temperature to 408 K (heating rate 10 K/min), 11 min at 408 K. Argon was applied as a carrier gas. The outlet streamline from the reactor to the gas chromatograph was heated at about 373 K to avoid condensation of reaction products.

3. Results and discussion

3.1. Characterization

SEM images of the materials used (Fig. 1) demonstrate the significant differences in morphology of the samples used.

The SEM image of Nb,Sb,V-O10 catalyst (Fig. 1a), i.e. the mechanical mixture of oxides V_2O_5, α-Sb_2O_4, T-Nb_2O_5 reveals different, irregular crystals of very small sizes from ~0.2 to ~1 μm. Fig. 1b is a scanning electron micrograph of Nb,(Sb-V)-O10 containing both $SbVO_5$ binary oxide and T-Nb_2O_5. Two types of crystals can be distinguished, large irregular "plates" ($SbVO_5$) and very small crystals (T-Nb_2O_5) of sizes below 0.25 μm. The SEM image of (Nb-Sb-V)-O10 (Fig. 1c) shows the presence of crystals of different sizes. The size of larger crystals is ~5 μm, whereas the sizes of the smaller crystals do not exceed 2 μm. The latter are similar to those presented in Ref. [18] for Sb(III)Sb(V)O_4 nanorods. One cannot exclude the presence of such species besides the ternary oxides characterized by bigger plate crystals. The SEM image of (Nb-V)-O25 (Fig. 1d) exhibits characteristic morphology of Nb_9VO_{25} crystals (elongated blocks) of several micrometers in size which is distinctly different from the morphology of (Nb-Sb-V)-O10.

XRD patterns (Fig. 2) confirm different phase composition of all catalysts applied in this work. In the diffraction pattern of Nb,Sb,V-O10 (Fig. 2a) only XRD lines characteristic of the orthorhombic oxides, V_2O_5 (JPDF card No: 77-2418), T-Nb_2O_5 (JPDF card No: 30-0873) and α-Sb_2O_4 (JPDF card No: 80-0231) are present. The diffractogram of Nb,(Sb-V)-O10 (Fig. 2b) contains a set of lines characteristic of $SbVO_5$ [17] besides the XRD lines characteristic of T-Nb_2O_5. The other two samples are characterized by XRD patterns typical of pure Nb_2SbVO_{10} [14] and Nb_9VO_{25} (JPDF card No: 49-0289) (Fig. 2c and d, respectively).

The structures of $SbVO_5$ and Nb_2SbVO_{10} are unknown so far. But we know that $SbVO_5$ crystallizes in the monoclinic system. The unit cell parameters refined by the least squares method [17] are as follows: a = 0.98647(5) nm, b = 0.49363(2) nm, c = 0.71281(4) nm, β = 109.797(8)°. The volume of such a unit cell is V = 0.3265893 nm^3, and the number of stoichiometric units per one unit cell Z = 4.

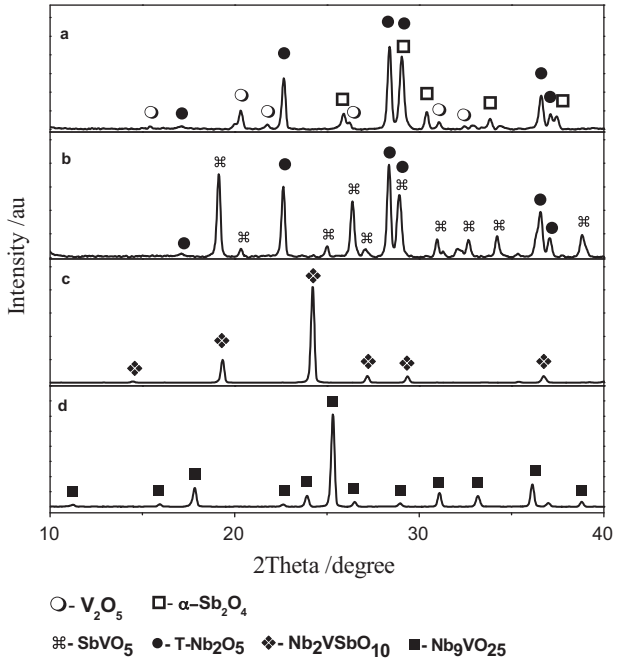

Fig. 2. X-ray diffraction patterns of (a) Nb,Sb,V-O10; (b) Nb,(Sb-V)-O10; (c) (Nb-Sb-V)-O10; (d) (Nb-V)-O25.

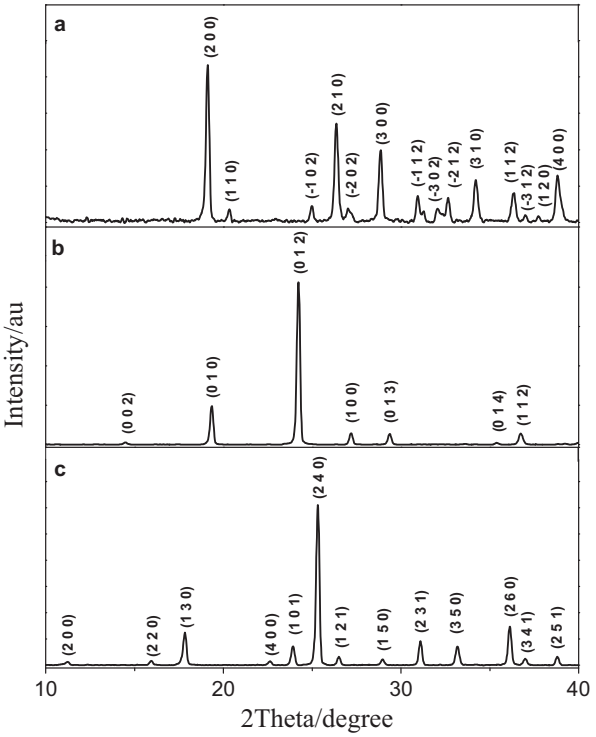

Fig. 3. X-ray diffraction patterns of (a) monoclinic $SbVO_5$; (b) orthorhombic Nb_2VSbO_{10}; (c) tetragonal Nb_9VO_{25}.

The parameters of the orthorhombic unit cell of Nb_2SbVO_{10} are the following: $a = 0.328143$ nm, $b = 0.458946$ nm, $c = 1.22476$ nm, $V = 0.184448$ nm^3 and $Z = 1$ [14].

In contrast to $SbVO_5$ and Nb_2SbVO_{10}, the structure of the Nb_9VO_{25} is well known [19]. The Nb_9VO_{25} crystallizes in the tetragonal system ($a = b = 1.5690$ nm, $c = 0.38172(9)$ nm, $V = 0.9397(3)$ nm^3, $Z = 2$) and its structure consists of 3×3 blocks of NbO_6 octahedra linked by corner-sharing VO_4 tetrahedra. The crystal structure of Nb_9VO_{25} is formed by two VO_4 tetrahedra and eighteen NbO_6 octahedra per unit cell. The XRD patterns of the referenced mixed oxides are shown in Fig. 3.

Infrared spectra allowed us to differentiate the vibrations of metal–oxygen bonds in the catalysts containing the same chemical composition and different morphology/structure properties (Fig. 4). A comparison of Fig. 4a and c clearly indicates differences in the metal–oxygen vibrations between the mechanical mixture of oxides (Nb,Sb,V-O10) and ternary oxide ((Nb-Sb-V)-O10). The band at 1023 cm^{-1} typical of stretching absorbance of the V=O bond [20] in highly distorted VO_6 octahedra building the layered structure of V_2O_5 [21,22] present in the Nb,Sb,V-O10 spectrum is observed as a shoulder in the spectrum of (Nb-Sb-V)-O10 ternary oxide. The new intense bands at 967 and 939 cm^{-1} in the spectrum of the latter sample seem to be a result of a shift to a lower frequencies of the band assigned to the V=O bond. Such a shift may be attributed to the interaction of vanadyl species with the different surroundings (Nb and Sb species). The other band typical of V_2O_5 crystalline phase at ca. 830 cm^{-1} originates from V-O-V vibrations [23–25] and it is intense in the spectrum of the mechanical mixture of metal oxides (Fig. 4a), whereas in the spectrum of the ternary oxide it is indicated as a shoulder (Fig. 4c). The strong band at 741 cm^{-1} (Fig. 4c) is typical of Sb_2O_3/Sb_2O_5 mixture [26] and its presence in the spectrum of (Nb-Sb-V)-O10 sample could suggest changes in the oxidation state of antimony in ternary oxide in comparison with its state in the mechanical mixture of metal oxides with Sb_2O_4 used. It can origin from Sb(III)Sb(V)O_4 phase suggested by SEM image. This band can be also attributed to stretching vibration of each metal (Nb, V, Sb)-oxygen bonds in tetrahedral neighbourhood. The other bands at 603 and 518 cm^{-1} in the spectrum (Fig. 4c) can be attributed to

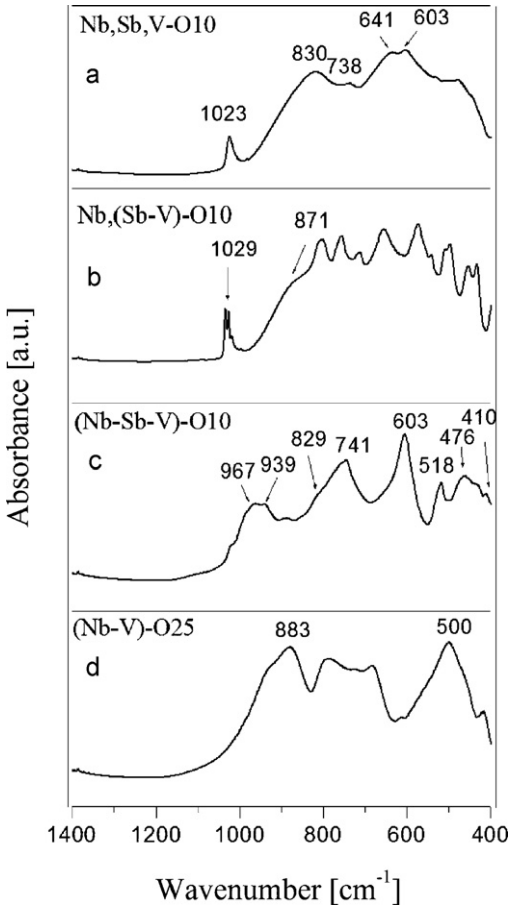

Fig. 4. FTIR spectra of catalysts used.

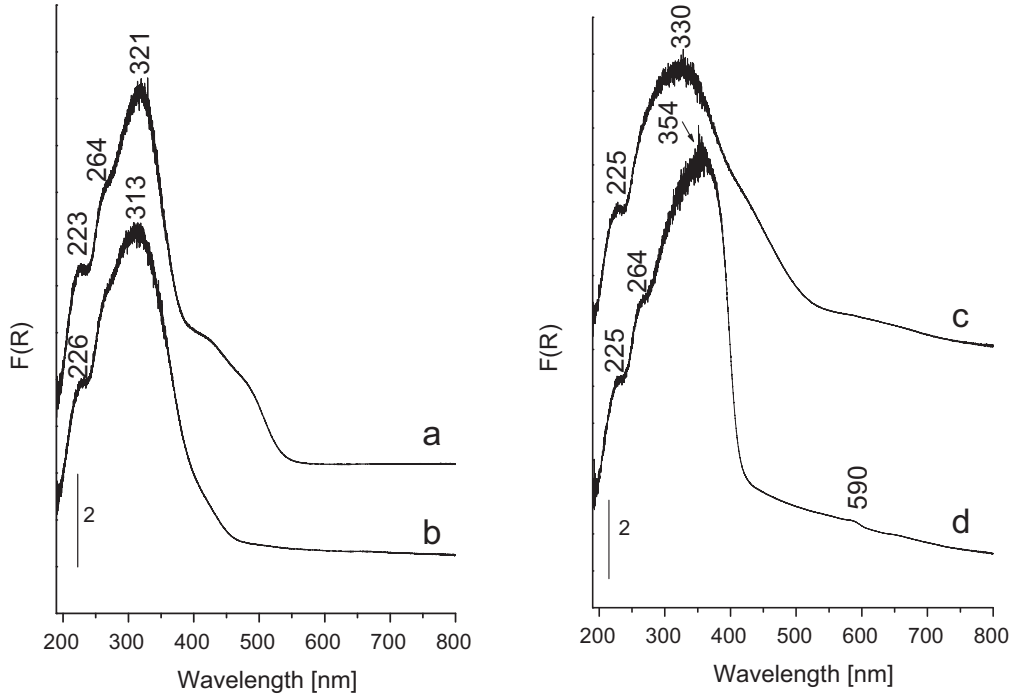

Fig. 5. UV–vis spectra of (a) Nb,Sb,V-O10; (b) Nb,(Sb-V)-O10; (c) (Nb-Sb-V)-O10; (d) (Nb-V)-O25.

O-Sb-O and Sb-O-Me (Me = V or Nb) stretching, respectively [27]. The Sb-O stretching bands in octahedral coordinated species (SbO_6) at 476 and 410 cm^{-1} are also present in the spectrum in Fig. 4c. The bands at 348 and 300 cm^{-1} (not shown here) are assigned to the deformation vibrations of M-O in NbO_4. The infrared spectrum of Nb_2SbVO_{10}, a compound of unknown structure, suggests that the lattice of this phase is formed by distorted tetrahedra of VO_4 and NbO_4 and octahedral SbO_6.

The spectrum of mechanical mixture Nb,(Sb-V)-O10 containing the $SbVO_5$ phase exhibits complex features (Fig. 4b). The spectrum of $SbVO_5$ phase has been already published [28] and the spectrum in Fig. 4b exhibits all bands characteristic of this phase. Some of them (at ca. 700, 600, and 500 cm^{-1}) cover the bands attributed to the niobia phase. A shoulder at ca. 871 cm^{-1} is typical of Nb_2O_5 phase. It has been proposed that $SbVO_5$ phase is built up from highly distorted polyhedra (SbO_6, VO_6 and VO_4) and has a layered structure [29].

The vibrational spectrum of compound Nb_9VO_{25} has been published in [15]. The crystal structure of the VNb_9O_{25} phase is built up of very symmetric VO_4 tetrahedra, as well as moderately and highly distorted NbO_6 octahedra [19].

UV–vis region examined is associated with the transfer of electron from oxygen to the transition metal. For all catalysts, low energy charge transfer, LCT, characteristic of the charge transfer between vanadium and oxygen, is evidenced in the 200–500 nm region. It is characteristic of V^{5+} cationic species [30]. The contribution of d-d transition of V^{4+} (d^1) that gives a broad band in the 550–800 nm region [30–33] is observed for the ternary (Nb-Sb-V)-O10 and binary (Nb-V)-O25 catalysts (a shoulder at ca 590 nm – Fig. 5). The presence of V^{4+} species was confirmed by ESR results [34] not shown here. The UV–vis band at ca 360 nm is very intense for (Nb-V)-O25 as typical of binary oxides (Fig. 5d), similarly as for rutile structure $Sb_{0.95}V_{0.95}O_4$. It shifts to a lower wavelength for ternary system of (Nb-Sb-V)-O10 (Fig. 5c). This band can be assigned to the electron transfer between V(V) and terminal (V=O) oxygen. The octahedral coordinated niobium species give a characteristic absorption band at ca. 330 nm [35,36]. Literature [37] describes different antimony oxides giving rise to the bands in the same region: assigned to Sb^{3+} (195–230 nm), Sb^{4+} and $Sb^{4.33+}$ (230–280 nm and 480 nm) and Sb^{5+} (300–340 nm). Unfortunately, UV–vis spectra do not allow us to distinguish these antimony species from niobium and vanadium phases. One can assign the band at 321 nm (Nb,Sb,V-O10) and 313 nm (Nb,(Sb-V)-O10) to both Sb^{5+} and Nb^{5+} octahedral coordinated species. Moreover, a broad band between 400 and 500 nm is assigned to the Sb_2O_4 phase. The ternary oxide (Nb-Sb-V)-O10 (Fig. 5c) presents a broad band centred at 330 nm with a tail up to ca 500 nm, which covers the electron transfers from oxygen to metals (Nb^{5+}, V^{5+}, Sb^{4+} and Sb^{5+}). The UV band at ca 225 nm present for all samples is characteristic of electron transfer in tetrahedral coordinated metal-oxide species (Nb^{5+} [38], V^{4+} [39] and Sb^{3+} [37]).

One can summarize the characteristic of oxides as follows. All the samples exhibit different morphology and different phase composition. The catalysts can be divided into two groups: (i) Nb,Sb,V-O10 and Nb,(Sb-V)-O10 characterized by multi phases and (ii) (Nb-Sb-V)-O10 and (Nb-V)-O25 having monophase. Vanadyl species (V=O), V-O-V and Sb_2O_4 were detected on the surface of the samples belonging to the first group, whereas in case of the (Nb-Sb-V)-O10 material O-Sb-O, Sb-O-Me and Sb_2O_3/Sb_2O_5 were found.

3.2. Catalytic activity

The cyclisation of acetonylacetone (AcOAc) was used as a test for acid/base properties. This reaction was proposed by Dessau [40]. The formation of 2,5-dimethylfuran (DMF) occurs at the acidic centres (Bronsted acid sites), whereas the production of 3-methyl-2-cyclopentenone (MCP) takes place at the basic centres (Scheme 1). On the basis of the MCP/DMF selectivity ratio, the sequence of basicity of the catalysts studied can be proposed. According to the literature [41] the basicity of the catalyst is demonstrated if MCP/DMF > 1. When MCP/DMF < 1 the catalyst exhibits mainly acidic properties, while MCP/DMF ~ 1 corresponds to the balanced acid–base properties. Table 2 presents the results obtained from this test reaction. The activity is low and almost the

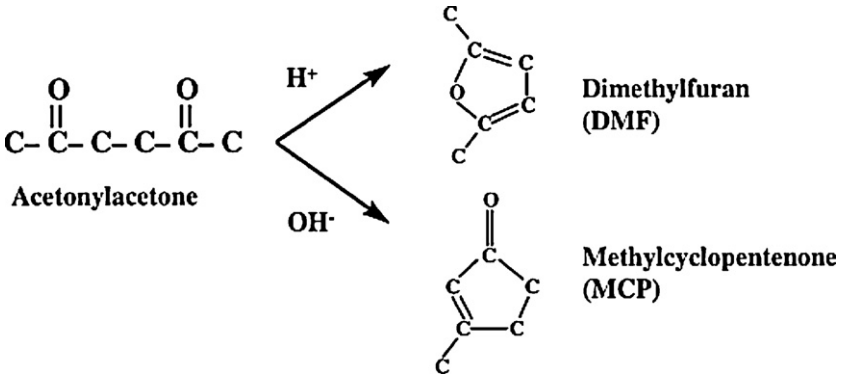

Scheme 1. Acetonylacetone transformation.

Table 2
The results of acetonylacetone (AcOAc) cyclisation at 623 K.

Catalyst	AcOAc conv. [%]	Selectivity [%]		MCP/DMF
		DMF*	MCP*	
Blank experiment	0	–	–	–
Nb,Sb,V-O10	7	45	55	1.22
Nb,(Sb-V)-O10	9	40	60	1.50
(Nb-Sb-V)-O10	8	49	51	1.04
(Nb-V)-O25	7	24	76	3.17

* MCP – 3-methyl-2-cyclopentenone; DMF – 2.5-dimethylfuran.

same for all samples. All, mechanical mixtures, ternary and binary oxides exhibit both acidity (DMF production) and basicity (MCP formation) on the surface. However, the selectivity differs significantly depending on the chemical composition of catalysts. Among the mechanical mixtures and ternary oxides (Nb-Sb-V)-O10 only Nb,(Sb-V)-O10 containing binary Sb-V system presents slightly higher basic than acidic properties (MCP/DMF = 1.5), whereas the binary oxide (Nb_9VO_{25}) exhibits significant domination of basicity demonstrated by the MPC/DMF ratio of 3.17.

The strongly basic character of (Nb-V)-O25 was confirmed by the results of 2-propanol decomposition carried out at 523 and 573 K (Fig. 6). The 2-propanol decomposition is a test reaction for identification of acidic (Brønsted or Lewis) and/or basic properties of solids [42]. Dehydration of alcohol to propene and/or di-isopropyl ether requires acidic centres (Lewis or BrØnsted), whereas the dehydrogenation to acetone occurs on the basic sites. Ether production requires the presence of pairs of Lewis acid–base centres. Some authors [43] have reported that acetone formation takes place on redox centres.

This test reaction allows estimation of surface properties of all materials used. Diagrams in Fig. 6 contain values of 2-propanol conversion at 523 and 573 K. It is clear that both mechanical mixture of three metal oxides (Nb,Sb,V-O10) and ternary ((Nb-Sb-V)-O10) oxide present almost the same very high activity in this reaction demonstrated by 2-propanol conversion of ca 90% at 573 K. At the lower temperature (523 K) the mechanical mixture of oxides is less active than the ternary oxide. Especially interesting is a significant difference in selectivity, which indicates differences in the surface properties. On both materials the main product is propene, which indicates highly acidic character of both samples. However, on ternary oxide a considerable amount of ether is also produced, which is not formed on mechanical mixture at 573 K. The formation of ether, which requires the presence of pairs Lewis acid–base centres, proves the existence of such pairs on ternary oxide and their higher activity than that in mixture of single oxides. Interestingly, the activity of two other samples is much lower, especially of those catalysts which do not contain antimony species. The latter sample ((Nb-V)-O25) catalyses the reaction mainly towards acetone formation. Significant amounts of acetone are also produced on Nb,(Sb-V)-O10. It is also very important to stress that both catalysts, Nb,(Sb-V)-O10 mechanical mixture and (Nb-V)-O25 contain binary oxides, antimony-vanadium and niobium-vanadium, respectively. It seems that the presence of binary oxides of different composition affects the activity in dehydrogenation of 2-propanol to acetone. Moreover, the presence of antimony species considerably increases the activity of the catalysts. This behaviour points out the role of antimony species as a promoter in catalytic reactions in which electron transfer is involved. Such a reaction is dehydrogenation of 2-propanol to acetone.

One more conclusion can be drawn from the results presented in Fig. 6. Antimony species are necessary for the creation of Lewis acid–base pairs responsible for the production of ether from 2-propanol. Generation of such active pairs is enhanced by the presence of the ternary oxide ((Nb-Sb-V)-O10) in comparison with mechanical mixture of oxides.

The difference in catalytic surface properties is even much more pronounced in the oxidation of methanol. This reaction is more complex and reflects the presence of acid centres involved in the chemisorption of methanol and active oxygen species. As follows from kinetic studies, the rate determining step of the selective oxidation of methanol is the abstraction of hydrogen from methyl group of methanol adsorbed. It is determined by the surface properties. Methoxy species formed in the first step can be adsorbed on oxygen vacancies in metal oxides (Lewis acid centres). The methoxy species adsorbed on a terminal M=O vacancy react towards formaldehyde by a transfer of a methyl H atom to the neighbouring M=O bond [44–46]. The methoxy species adsorbed on the bridged oxygen (M-O-M) vacancy sites are likely to form dimethyl ether, dimethoxymethane (methylal), and methyl formate, which requires the presence of additional Lewis acid sites [44]. Thus, most authors working on the selective oxidation of methanol considered a significant role of acidity and basic oxygen species in the metal oxide catalysts. Finally, basicity is responsible for total oxidation of methanol to CO_2 as proposed by Tatibouet [47]. The total oxidation of methanol to carbon dioxide can proceed also in the direct oxidation of methanol involving electrophilic oxygen species (radical species) [48] or by the readsorption of HCHO and its secondary reaction as proposed by Wachs and Kim [49]. In this study a good correlation of the acetone formation in 2-propanol dehydrogenation and CO_2 generation in methanol oxidation suggests the significant role of basic oxygen in the total oxidation of methanol.

Fig. 7 reveals a very high selectivity to formaldehyde of all catalysts containing three metals, but the highest selectivity to this product is reached on ternary oxide ((Nb-Sb-V)-O10) and a

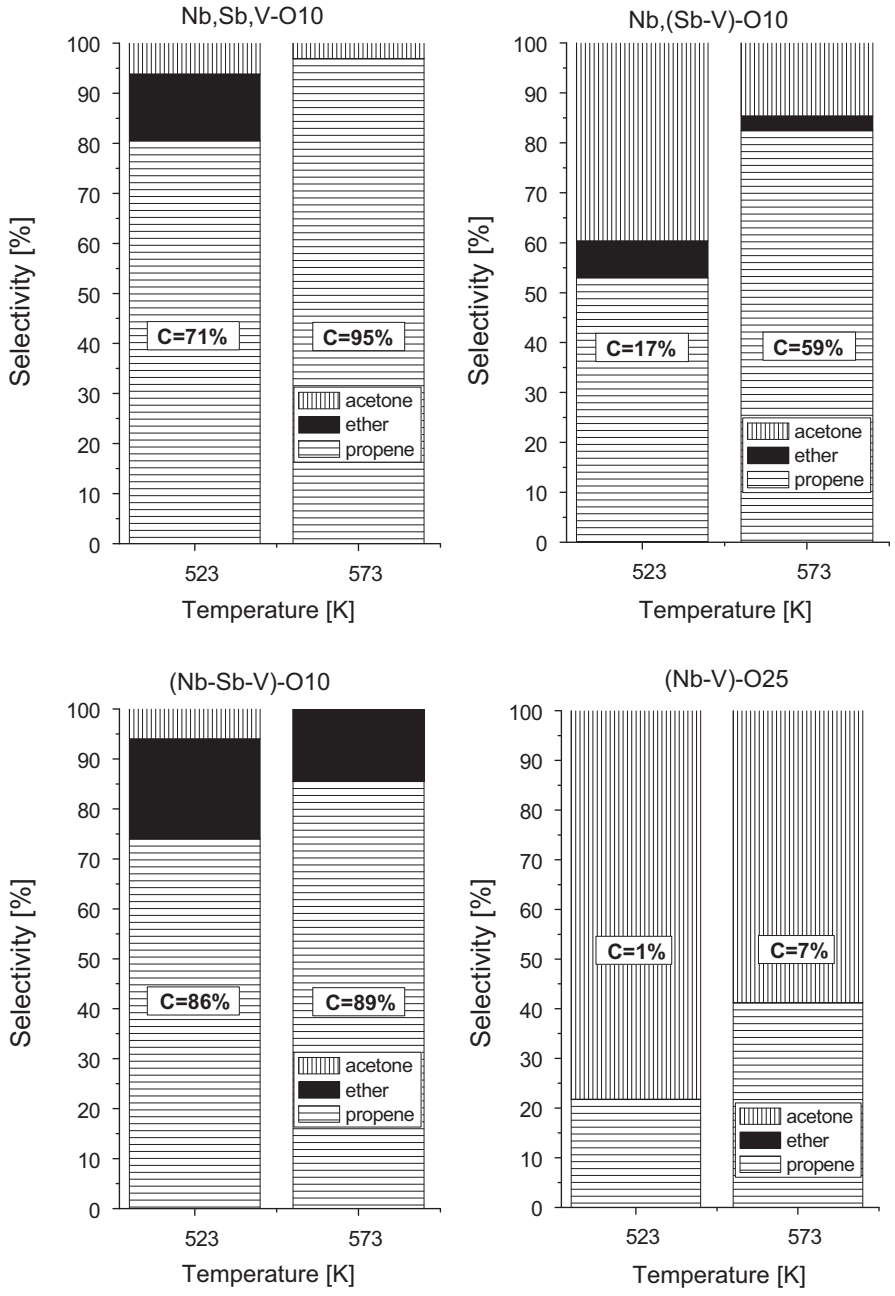

Fig. 6. The results of 2-propanol decomposition at 523 and 573 K (C means conversion of 2-propanol).

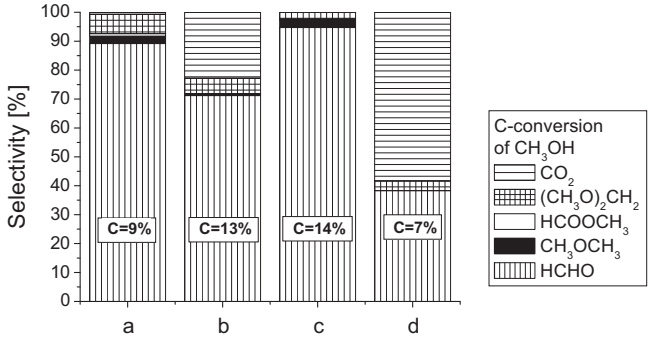

Fig. 7. The results of methanol oxidation (Ar/O_2/MeOH (88/8/4 mol%)) at 523 K: (a) Nb,Sb,V-O10; (b) Nb,(Sb-V)-O10; (c) (Nb-Sb-V)-O10; (d) (Nb-V)-O25.

mixture of three metal oxides (Nb,Sb,V-O10). For the same methanol conversion the selectivity to formaldehyde is slightly higher on ((Nb-Sb-V)-O10) catalyst (Table 3). In spite of significant differences in morphology and different vibrational metal-oxide properties of ternary oxide and mixture of single oxides of the same chemical composition, the selectivity in methanol oxidation is not considerably different. Interestingly, the samples containing binary oxides, Nb,(Sb-V)-O10 and (Nb-V)-O25 are highly active in the total oxidation of methanol to CO_2, which is especially characteristic of the latter material. It is commonly agreed that CO_2 formation requires the presence of basic sites on the catalyst surface. Thus, methanol oxidation confirms the results of both test reactions, acetonylacetone cyclisation and 2-propanol decomposition, which indicate strongly basic character of samples containing binary oxides.

Table 3
The results of methanol oxidation (Ar/O_2/MeOH (88/8/4 mol%)) for the same methanol conversion.

Catalyst	Temp [K]	MeOH conv [%]	Selectivity [%]				
			HCHO	CH_3OCH_3	$HCOOCH_3$	$(CH_3O)_2CH_2$	CO_2
Blank experiment	523	0	–	–	–	–	–
Nb,Sb,V-O10	523	10	90	2	2	5	1
Nb,(Sb-V)-O10	523	11	70	1	0	5	24
(Nb-Sb-V)-O10	523	11	95	2	1	2	Traces
(Nb-V)-O25	573	10	37	0	0	3	60

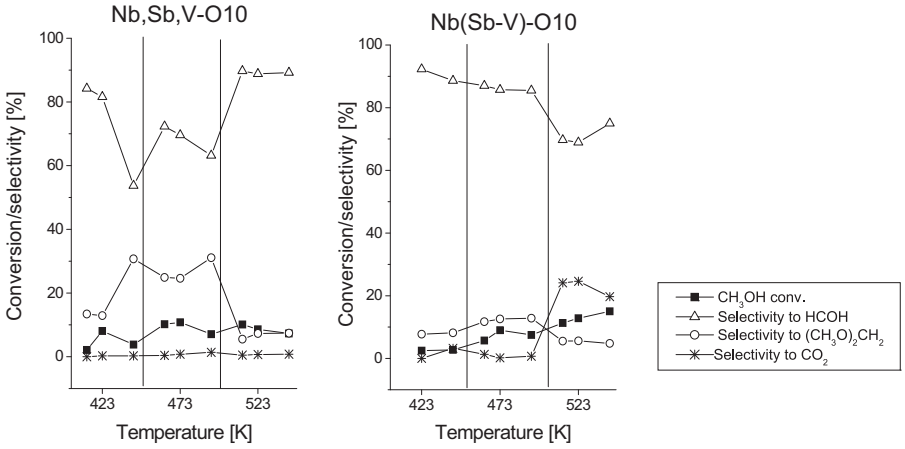

Fig. 8. Methanol oxidation at different temperatures (Ar/O_2/MeOH (88/8/4 mol%)).

The difference between Nb,Sb,V-O10 and Nb,(Sb-V)-O10 is well illustrated in Fig. 8 presenting the conversion of methanol and selectivity of its oxidation at different temperatures. For the first catalyst the increase in the reaction temperature from 473 to 523 K results in an increase in the selectivity to formaldehyde and a decrease in the selectivity to dimethoxymethane. The latter is formed if chemisorbed formaldehyde is held strongly enough at the acidic centre and can interact with the following methanol molecules. An increase in the reaction temperature causes a faster desorption of formaldehyde and therefore the formation of dimethoxymethane decreases. In contrast, when Nb,(Sb-V)-O10 catalyst is used, the increase in the reaction temperature from 473 to 523 K causes a decrease in the selectivity to formaldehyde and to dimethoxymethane but significantly enhances the selectivity to CO_2. Carbon dioxide is formed at higher temperature by the total oxidation of formaldehyde with the participation of basic oxygen from the catalyst surface.

4. Conclusions

Acid/base and redox properties of the oxide catalysts containing Nb, Sb, V, O (atomic ratio: 2:1:1:10) strongly depend on the presence of binary oxide, which significantly enhances the basicity of the catalysts. The highest basicity was found for pure binary oxide Nb_9VO_{25}. Basic character of the catalysts containing binary oxides was revealed on the basis of acetone formation in 2-propanol dehydrogenation, methylcyclopentenone production in acetonylacetone cyclisation and total oxidation to CO_2 in the reaction between methanol and oxygen.

Acid–base and redox character of ternary oxide ((Nb-Sb-V)-O10) and the mechanical mixture of single oxides (Nb,Sb,V-O10) is not significantly different. The main difference is in the generation of more active Lewis acid–base pairs in ternary oxide, which is demonstrated by the production of ether in the intermolecular dehydration of 2-propanol. The activity of such pairs was not found in mechanical mixture of single metal oxides in the reaction performed at 573 K.

Finally the role of antimony should be stressed. The catalyst without Sb exhibits much lower activity in the transformation of both alcohols. It points out the promoting character of antimony species in the reactions involving electron transfers.

Acknowledgements

This work has been performed in the framework of a D36/0006/06 COST program. Polish Ministry of Science and Higher Education (Projects nos: N N 204 016439 and N N204 153740) is acknowledged for a financial supports.

References

[1] B.M. Weckuysen, D.E. Keller, Catal. Today 78 (2003) 25.
[2] M.O. Guerrero-Pérez, M.A. Vicente, J.L.G. Fierro, M.A. Bañares, Chem. Matter. 19 (2007) 6621.
[3] M.O. Guerrero-Pérez, M.V. Martínez-Huerta, J.L.G. Fierro, M.A. Bañares, Appl. Catal. A Gen. 298 (2006) 1.
[4] M.O. Guerrero-Pérez, L. José, J.A. Rivas-Cortés, J.L.G. Delgado-Oyagüe, M.A. Fierro, Bañares, Catal. Today 139 (2008) 202.
[5] R. Grasselli, Catal. Today 99 (2005) 25.
[6] M.O. Guerrero-Pérez, J.L.G. Fierro, M.A. Vicente, M.A. Banares, J. Catal. 206 (2002) 339.
[7] H. Zhang, Z. Liu, Z. Feng, C. Li, J. Catal. 260 (2008) 295.
[8] L.T. Weng, P. Ruiz, B. Delmon, Stud. Surf. Sci. Catal. 72 (1992) 339.
[9] X. Gao, I.E. Wachs, M.S. Wong, J.Y. Ying, J. Catal. 203 (2001) 18.
[10] K. Routray, W. Zhou, C.J. Kiely, I.E. Wachs, ACS Catal. 1 (2011) 54.
[11] I.E. Wachs, Appl. Catal. A Gen. 391 (2011) 36.
[12] M.O. Guerrero-Pérez, M.A. Bañares, Catal. Today 142 (2009) 245.
[13] H. Golinska, P. Decyk, M. Ziolek, Catal. Today 169 (2011) 242.
[14] E. Filipek, M. Piz, J. Therm. Anal. Calorim. 101 (2010) 447.
[15] P. Tabero, E. Filipek, M. Piz, Cent. Eur. J. Chem 7 (2) (2009) 222.
[16] E. Filipek, J. Therm. Anal. Calorim. 56 (1999) 159.
[17] E. Filipek, Solid State Sci. 8 (2006) 577.
[18] T. Ji, M. Tang, L. Guo, X. Qi, Q. Yang, H. Xu, Solid State Commun. 133 (2005) 765.
[19] M.T. Casais, E. Gutierrez-Puebla, M.A. Monge, I. Rasines, C.J. Ruiz-Valero, Solid State Chem. 102 (1993) 261.
[20] S. Albonetti, G. Blanchard, P. Burattin, T.J. Cassidy, S. Masetti, F. Trifiro, Catal. Lett. 45 (1997) 119.

[21] R. Enjalbert, J. Galy, Acta Cryst. C 42 (1986) 1467.
[22] L. Abello, E. Husson, Y. Repelin, G. Lucazeau, Spectrochim. Acta A 39 (1983) 641.
[23] M. Baltes, K. Cassiers, P. van der Voort, B.M. Weckhuysen, R.A. Schoonheydt, E.F. Vansant, J. Catal. 197 (2001) 160.
[24] L.D. Frederickson, D.M. Hansen, Anal. Chem. 35 (1968) 813.
[25] B.M. Reddy, I. Ganesh, B. Chowdry, Catal. Today 49 (1999) 115.
[26] M. Bowker, C.R. Bicknell, P. Kerwin, Appl. Catal. A Gen. 136 (1996) 205.
[27] F. Ivars, B. Solsona, E. Rodriguez-Castellon, J.M. Lopez Nieto, J. Catal. 262 (2009) 35.
[28] E. Filipek, The Synthesis and Physicochemical Properties of New Phases in the Systems Oxides V2O5, MoO3, α-Sb2O4, Editorial Office – Szczecin University of Technology, 2007, ISBN 978-83-7457-025-1.
[29] E. Filipek, P. Tabero, Thermal expansion and IR spectra of SbVO5, in: 8th Conference on Solid State Chemistry (SSC), Bratislava, Slovakia, Book of Abstracts 190, 6–11 July, 2008.
[30] D. Hong, V.P. Vislovskiy, Y. Hwang, S.H. Jhung, J.S. Chang, Catal. Today 131 (2008) 140.
[31] C. Tellez, M. Abon, C. Mirodatos, J. Santamaria, J. Catal. 195 (2000) 113.
[32] E.V. Kondratenko, M. Baerns, Appl. Catal. A Gen. 222 (2001) 133.
[33] G. Catana, R. Ramachandra Rao, B.M. Weckhuysen, E. Pascal Van Der Voort, R.A. Vansant, Schoonheydt, J. Phys. Chem. B 102 (1998) 8005.
[34] J. Typek, G. Zolnierkiewicz, A. Cyran, K. Wardal, E. Filipek, M. Piz, Proc. Conf. FNMA11 – Functional and Nanostructured Materials, Szczecin, Poland, 6–9 Sept., 2011.
[35] M. Nashimura, K. Asakura, Y. Iwasawa, J. Chem. Soc. Chem. Commun. 15 (1986) 1660.
[36] M. Trejda, A. Wojtaszek, A. Floch, R. Wojcieszak, E.M. Gaigneaux, M. Ziolek, Catal. Today 158 (2010) 170.
[37] H. Matsumura, K. Okumura, T. Shimamura, N. Ikenaga, T. Miyake, T. Suzuki, J. Mol. Catal. A 250 (2006) 122.
[38] M. Trejda, A. Tuel, J. Kujawa, B. Kilos, M. Ziolek, Micropor. Mesopor. Mater. 110 (2008) 271.
[39] T. Blasco, A. Galli, J.M. Lopez Nieto, F. Trifiro, J. Catal. 169 (1997) 203.
[40] R.M. Dessau, Zeolites 10 (1990) 205.
[41] J.J. Alcaraz, B.J. Arena, R.D. Gillespie, J.S. Holmgren, Catal. Today 43 (1998) 89.
[42] A. Gervasisni, J. Fenyvesi, A. Auroux, Catal. Lett. 43 (1997) 219.
[43] C. Lahousse, J. Bachelier, J.C. Lavalley, H. Lauron-Pernot, A.M. Le Govic, J. Mol. Catal. 87 (1994) 329.
[44] C.H. Bartholomew, R.J. Farrauto, Fundamentals of Industrial Catalytic Processes, John Wiley & Sons, Inc., 2005, pp. 578–597.
[45] R.Z. Khaliullin, A.T. Bell, J. Phys. Chem. B 106 (2002) 7832.
[46] J. Dobler, M. Pritzsche, J. Sauer, J. Am. Chem. Soc. 127 (2005) 10861.
[47] J.M. Tatibouet, Appl. Catal. A Gen. 148 (1997) 213.
[48] M. Muhler, in: G. Ertl, H. Knozinger, J. Weitkamp (Eds.), Handbook of Heterogeneous Catalysis, VCH, 1997, pp. 2274–2283.
[49] T. Kim, I.E. Wachs, J. Catal. 255 (2008) 197.